ISSN 1064-2269, Journal of Communications Technology and Electronics, 2018, Vol. 63, No. 2, pp. 95–103. © Pleiades Publishing, Inc., 2018.
Original Russian Text © G.A. Kraftmakher, V.S. Butylkin, Yu.N. Kazantsev, V.P. Mal'tsev, 2018, published in Radiotekhnika i Elektronika, 2018, Vol. 63, No. 2, pp. 107–118.

ELECTRODYNAMICS AND WAVE PROPAGATION

Specificities of the Microwave Reflection Coefficients of Magnetically Excited Chiral and Ring Conductive Elements for Separation of Magnetic and Electric Responses and Broadband Matching of Radio Absorbing Composites

G. A. Kraftmakher*, V. S. Butylkin, Yu. N. Kazantsev, and V. P. Mal'tsev

Institute of Radio Engineering and Electronics (Fryazino Branch), Russian Academy of Sciences, Fryazino, Moscow oblast, 141190 Russia

**e-mail: gkraft@ms.ire.rssi.ru*

Received October 19, 2016

Abstract—Distinctive features of the resonance responses of the reflection of microwaves from conducting double and single split-ring resonators, making it possible to distinguish between the magnetic and electric responses and identify the magnetic response of elements of different shapes, are studied experimentally in a rectangular waveguide and numerically in free space. It is shown that the specificities of the frequency dependence of the magnetic response can be used for broadband matching of radio absorbing composites.

DOI: 10.1134/S1064226918020043

INTRODUCTION

The interest in metamaterials based on chiral conducting elements smaller than the wavelength is largely due to the unique effects caused by resonance ring currents.

Ring currents can be induced in elements by alternating magnetic (h, magnetic excitation) or electric (E, electric excitation) fields, depending on their orientation. The current induced by a magnetic field h creates alternating magnetic and electric dipole moments, while the magnetic moment contributes to the permeability μ and the electric moment contributes to the chirality parameter that affects the magnetic induction. If a ring current is induced by an electric field E, the magnetic and electric dipole moments are formed but, in this case, the electric moment contributes to the permittivity ε and the magnetic moment contributes to the chirality parameter, which influences the electric induction. In addition, in chiral elements, the electric field can induce resonance currents similar to the currents in ordinary dipoles. The magnetic response or magnetic resonance will be understood as a response to magnetic excitation. The resonance effects excited by currents similar to dipole currents will be called a "dipole resonance" (DR).

The unique properties of metamaterials and their possible applications are discussed in [1].

The discrimination between different resonance effects is necessary for identifying the magnetic response, which is required in the development of artificial magnetic materials, "left-handed" media [2, 3], and antireflection absorbers for achieving equal values of the permittivity and permeability [4–9]. The existing methods of identifying the responses, based on the analysis of the transmission spectra [10, 11], are complex and unreliable, since they require special samples or evanescent waveguide structures.

In addition, it is necessary to develop methods for discrimination and identification of the type of excitation, taking into account the large set of elements of various types, the multitude of resonances, and difficulties of direct measurements of magnetic and electric parameters [12]. The exact resonator method allows direct measurements but requires special samples satisfying the conditions for the applicability of perturbation theory [13]. In [14], the distinctive features of the magnetic and electric responses of the reflection from planar double split-ring resonators (PDSRRs) were found and it was shown that these features can be used not only for identifying the magnetic response but also for matching radio absorbers. In [15], the possibility of compensating the reflection from a radio-absorbing material not on the basis of traditional quarter-wave effects by capacitive or inductive arrays [16, 17] but using an array of PDSRRs was demonstrated experimentally and numerically.

The aim of this work is to implement the elements and structures and to study the distinctive features of microwave reflection responses in order to make it possible to identify the type of excitation (by an alternating magnetic or electric field) of resonances in con-

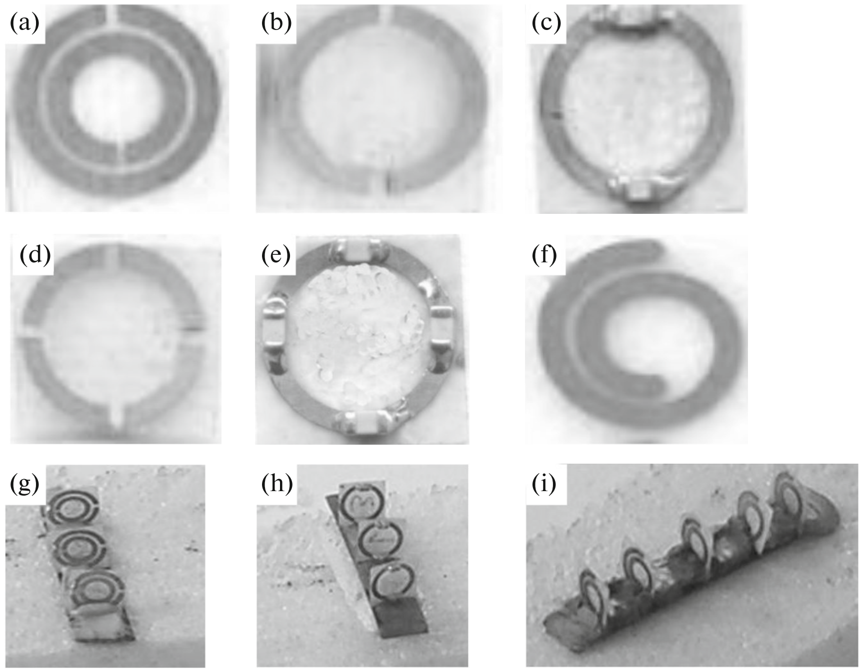

Fig. 1. Elements under study: (a) a planar double split-ring resonator PDSRR, (b) a single split-ring resonator with two symmetric splits, (c) with two symmetric splits closed by capacitors, (d) a single split-ring resonator with four splits, (e) a single split-ring resonator with four splits closed by capacitors, (f) a planar spiral, and (g–i) rows of split ring resonators and spirals.

ducting chiral and ring elements for elements of different shapes and to elucidate the possibility of new applications of the magnetic response for the broadband compensation of reflections from absorbing composites.

1. METHODS OF STUDY. CHIRAL DOUBLE SPLIT-RING RESONATORS

Figure 1 shows photographs of the chiral and ring elements (with an outer diameter of 6.6 mm) under study, and Fig. 2 shows radio absorbing metastructures with ring elements for matching to free space.

Let us demonstrate the methods and the results of measurements and calculations on the example of planar double split-ring resonators (PDSRRs) (Fig. 1a), since the processes of resonance excitation in such resonators were analytically and numerically studied [18, 19]. The PDSRRs are not chiral in the geometric sense, but we will classify them as chiral elements since they involve the magnetoelectric interaction and the media based on them are characterized by a nonzero chirality tensor. We measure the microwave responses of elements and structures placed in rectangular waveguides. The calculation is performed for an infinite array of elements in free space. The measured elements or structures are indicated on the corresponding insets to the experimental curves. The calculated curves contain insets with elements united into infinite arrays.

Let us describe the succession of actions in the method of study proposed. We measure the reflection coefficients R and the transmission coefficients T in a rectangular waveguide using voltage standing wave ratio meters: P2-58, a 48 × 24-mm waveguide (3–5.5 GHz); P2-59, a 35 × 15-mm waveguide (5.3–7.6 GHz); and P2-61, a 23 × 10-mm waveguide (7.5–12 GHz). We use the standing-wave mode with a metal plug and a traveling-wave mode with a matched load. A PDSRR (Fig. 3a) is placed at the center of the rectangular waveguide in different orientations relative to the incident field components (Fig. 3b). For each of the orientations (***1***, ***2***, ***3***, and ***4***) of the PDSRR, we know the type of excitation of the resonance ring current (ring resonance, RR). In particular, magnetic h-excitation is achieved in orientation ***1***; orientation ***2*** allows the magnetic and electric h- and E-excitations; in orientation ***3***, the RR is not excited; the electric E-excitation is achieved in orientation ***4***. The corresponding measured frequency dependences of the reflection coefficient R_m for orientations ***1*** and ***4*** in the standing-wave mode are shown in Figs. 3c and 3d. In Fig. 3c, the resonant minimum is manifested when the PDSRR has orientation ***1*** (the h-excitation) and is situated at a distance $s = 0$ from the metal plug, at an antinode of the magnetic field h. The resonance vanishes at the minimum of the field h, when the PDSRR is situated at a distance of $s = \lambda/4$ from the plug. At $s = \lambda/4$, the resonance is observed in orientation ***4*** (the E-excitation) at the maximum of the field E and disappears at $s = 0$, at the minimum of E (Fig. 3d). This simple method of

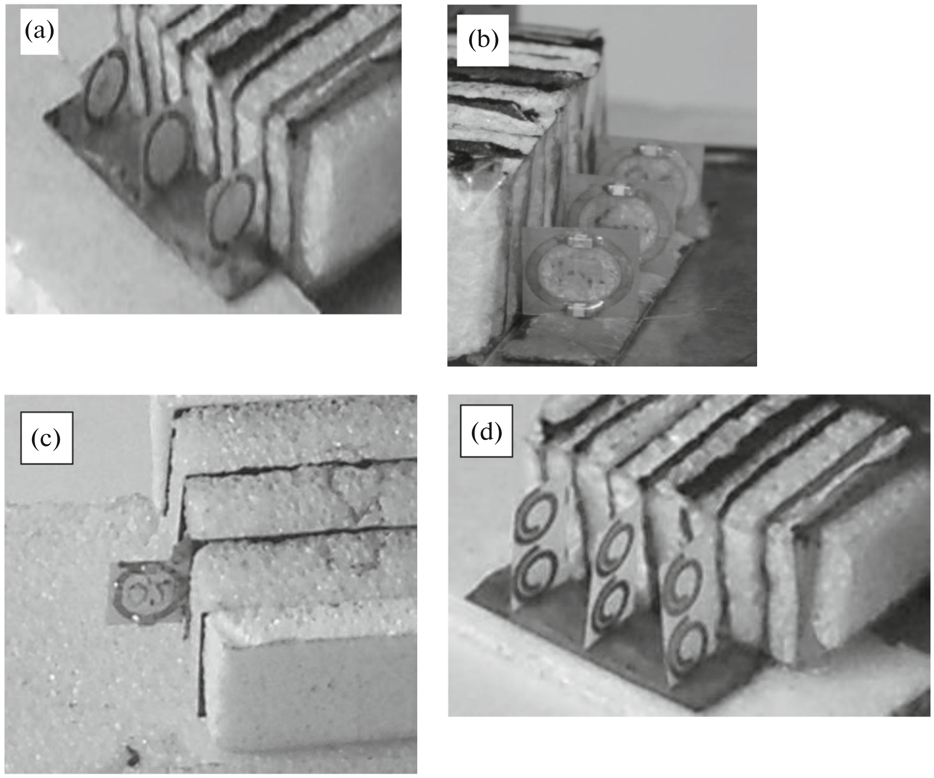

Fig. 2. Absorbing composites with matching elements in the form of (a) single double split-ring resonators, (b) single split-ring resonators loaded with capacitors; (c) single split-ring resonators loaded with capacitors; and (d) planar 1.5-turn spirals.

separating the magnetic and electric excitations requires samples that are thin in comparison with the wavelength, so that, at the antinode of the magnetic (electric) field of the wave, the sample be not affected by the electric (magnetic) field.

In the traveling-wave mode, the resonant effects manifest themselves as a resonance dip (minimum) of the frequency curves of the transmission coefficient, associated with the resonance maximum of the reflection coefficient curve. Such curves are typical of composites based on resonant chaotically arranged elements. However, in the case of oriented chiral elements, including solitary elements (as will be shown below), the resonance reflection curves have a more complex form: along with the resonance maximum, an associated resonance minimum with the position of depending on the type of excitation is observed.

The experimental frequency dependences of the reflection coefficient R in the region of the RR in the traveling-wave mode are shown in Fig. 3d; they are cardinally different for different orientations. Along with the resonance maxima (frequency $f_{\max}$ = 6.3 GHz), we observe resonance minima at frequencies lower (6 GHz), in the case of the magnetic h-excitation in orientation ***1***, and higher (6.5 GHz) in the case of the electric E-excitation in orientation ***4***. In orientation ***2***, both h- and E-excitation can take place; in this case, we observe blurred minima of the R curve. Orientation ***3*** does not allow RR excitation, and the resonance effect on the R curve is absent. An important point is the preservation of a sufficiently high reflection above the resonance maximum under magnetic excitation.

The calculation results are presented in Figs. 4a–4c. As in the experiment, the resonance dependences R in the region of the RR are close to 6.5 GHz, where the shape of the resonance curve essentially depends on the excitation, in contrast to the resonance dip of the transmission coefficient T (Fig. 4c). In addition, at higher frequencies (15–20 GHz), dipole resonances (DRs) with specificities of the electric excitation are manifested. The resonant reflection curves in the region of the RR under the electric excitation and in the region of the DR are identical; they exhibit resonance minima above the resonance maximum corresponding to the dip of the transmission coefficient T. It should also be noted that the phase of R varies slowly, passing through zero under magnetic excitation, while, under electric excitation, the phase changes abruptly (see Fig. 4b).

The difference in the frequency characteristics makes it possible to identify the type of excitation and to separate the magnetic and electric resonance responses, and the proposed approach can be applied to inclusions of a wide variety of forms. Acute minima in the frequency dependence of R below the resonance maxima were observed experimentally for arrays of

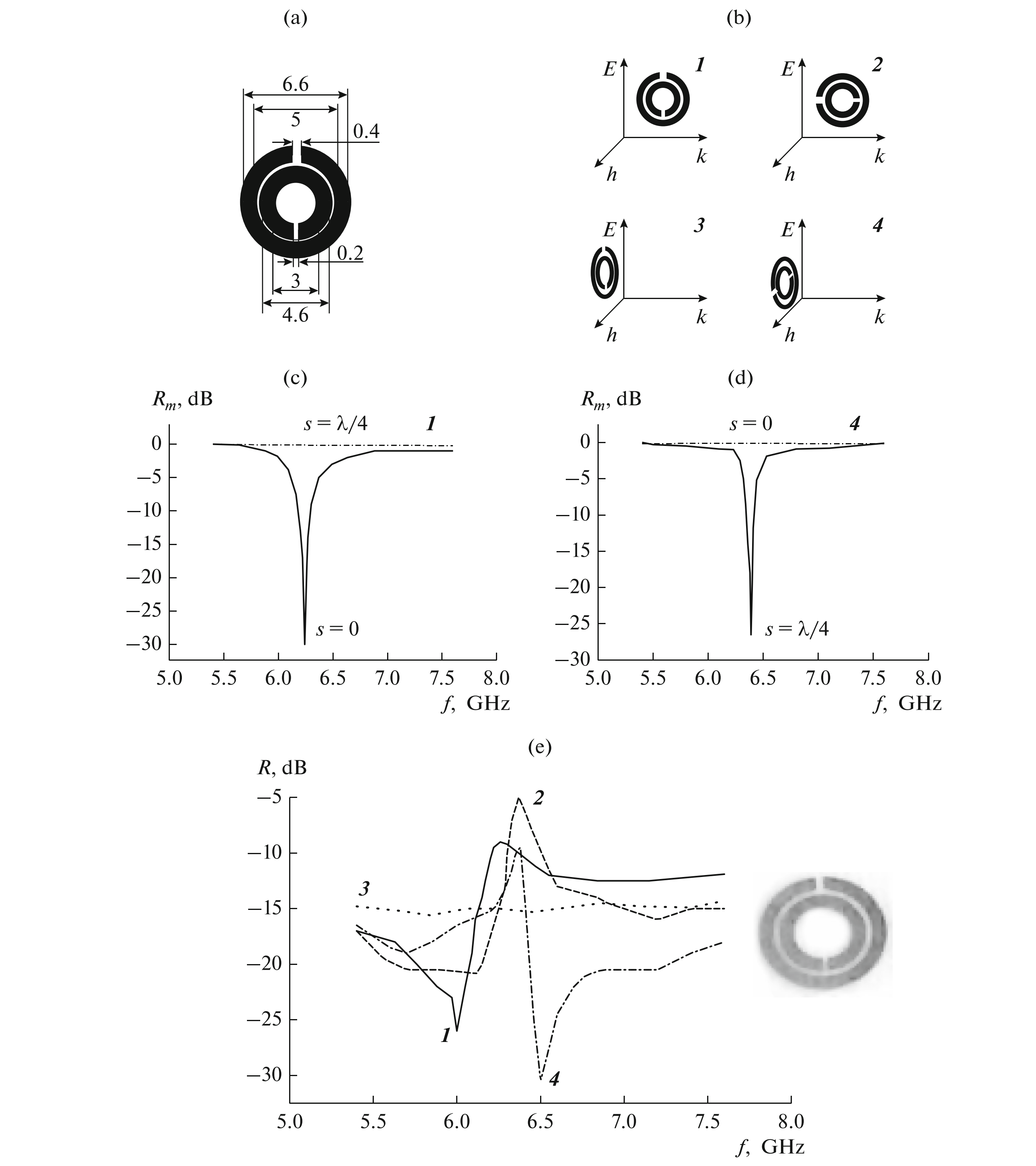

Fig. 3. (a) Geometry of a planar double split-ring resonator PDSRR and (b) the studied orientations of the PDSRR relative to the wave vector k and the fields h and E of the incident electromagnetic wave; measured frequency dependences of the reflection coefficients R (traveling wave) and R_m (standing wave) in a rectangular waveguide in the region of the ring resonance: R_m in orientations (c) ***1*** and (d) ***4*** and (e) R in orientations ***1–4*** (different excitation of the resonance).

PDSRRs and planar spirals oriented under a magnetic excitation and placed in free space between a transmitting and receiving waveguides along the direction of propagation [20].

The magnetic excitation is of interest because it provides microwave artificial magnetism [21, 22], which is required for creating artificial composites with magnetic properties [23, 24], "left-handed media" [2, 25] and, as will be shown below, can be used for new applications. In particular, the presence of thermal losses limits the use of the magnetic response for the left-handed media but is attractive for creating absorbers of electromagnetic radiation with low reflection. Finding the features of the frequency characteristics of R (a smooth phase variation near the zero value and preserving a large value above the resonance frequency) opens an aspect of the problem of absorption not discussed earlier: the possibility of broadband compensation of frequency-dependent reflections from traditional absorbing composites based on resistive filaments or films. The compensation is achieved by providing equal values of antiphase reflections from the composite and from a closely located array of resonant elements excited by the magnetic field of the wave above their resonance frequency. The possibility of compensating reflections by means of PDSRRs was demonstrated in [14, 15].

Below, it will be shown that the proposed method for identifying the resonance magnetic response can be used for inclusions of different shapes, e.g., single split-ring resonators with two and four splits and also planar 1.5-turn spirals. The change in the shape and size of elements changes the electrodynamic parameters and expands the range of possible applications. To this end, single split-ring resonators with symmetric splits and planar spirals were fabricated. The dimensions of the elements (a diameter of 6.6 mm) were chosen to observe resonances in a given range of wavelengths. The absorbing composite (with a length of 80–90 mm, the cross section corresponding to the complete filling of the waveguide, the transmission coefficient T = 30 dB) consisted of several layers of carbon-containing paper (with a thickness 0.07 mm and ε' = 15) separated by layers of polystyrene foam (with a thickness of 1, 2, and 4 mm and ε' = 1.02). For the approbation, the frequency dependences of R (in the traveling-wave mode) and R_m (in the standing-wave mode with a metal plug) for the elements at different orientations relative to the components of the incident electromagnetic field were measured in a rectangular waveguide. Resonance region were found, and the distinctive features were analyzed. The magnetic response was identified. The possibilities of matching were determined by measuring the R of the absorbers with and without matching elements. Frequency regions with dips of reflection when the elements of the array were matched under a magnetic excitation were found. A numerical calculation for free space was carried out.

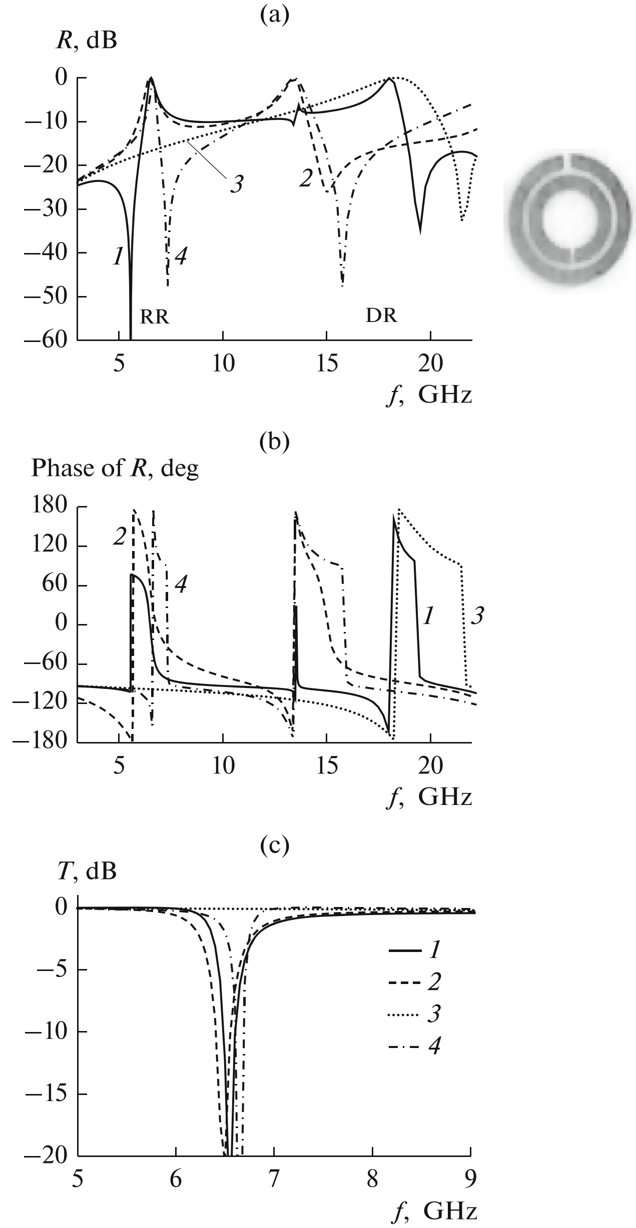

Fig. 4. Calculated dependences of the (a) reflection coefficients R and (c) transmission coefficient T for a periodic array of PDSRRs in free space for different orientations of the rings, the lattice period being of 13 mm; (b) the phase of R.

2. SINGLE SPLIT-RING RESONATORS

Let us show that the characteristic features of the magnetic response of reflection are observed for single split-ring resonators with symmetric splits and a load with capacitances of 0.1 pF (see Figs. 1b and 1c). A ring was placed at the center of a rectangular waveguide. In orientation ***1*** of the ring (see Fig. 3a), RRs were excited by a magnetic field h and an electric field E. The frequency dependences of the reflection coefficient R measured in the region of the RR with orientation ***1*** are shown in Fig. 5a. These dependences are qualitatively similar to those for PDSRRs. In particular, in the traveling-wave mode, along with the maximum of the reflection coefficient R (near 10 GHz), which preserves large values at higher frequencies, a resonance minimum at frequencies near 9 GHz is

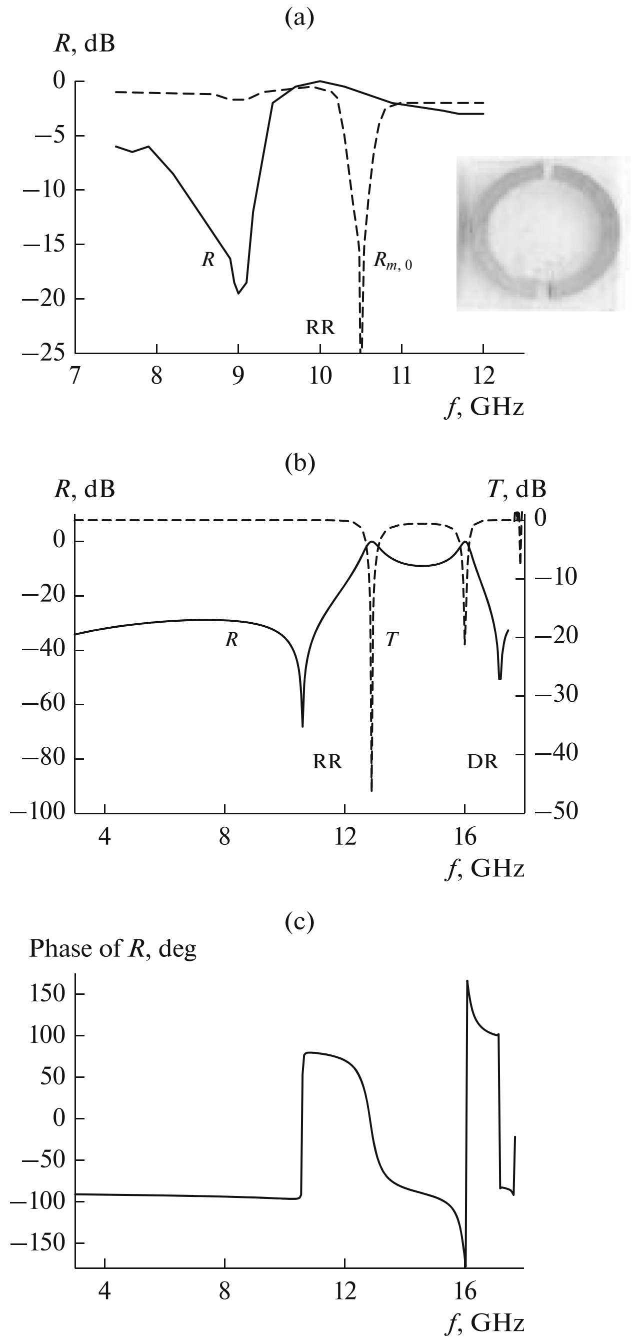

Fig. 5. Frequency dependences of the (a) reflection coefficients R and (b) transmission coefficient T of a single split-ring resonator with two splits in the orientation ***1***; (a) experiment in the traveling-wave mode (curve R) and in the standing-wave mode when the ring is placed near a metal plug, $s = 0$ (curve $R_{m,0}$) in the region of the ring resonance RR; (b, c) calculated dependences of the reflection coefficients R (magnitude and phase) and transmission coefficient T for a periodic array of rings in free space.

observed. In the-standing wave mode, when the ring resonator was placed on a metal plug, a resonance dip of $R_{m,0}$ was observed at the maximum of the magnetic field h. The calculation results for the absolute value and phase of R in the traveling-wave mode are shown in Fig. 5b and 5c. The regions of the RR near 12 GHz and of the DR near 16 GHz with distinctive features are presented. Under a magnetic excitation the RR, along with the maximum of reflection, a resonance minimum below the frequency of the maximum with a large value of R preserved at higher frequencies was observed. A typical feature of the electric excitation of the DR is a resonance minimum of reflection above the frequency of the maximum. The maxima of the reflection coefficient R correspond to resonance dips of the transmission coefficient T, regardless of the type of excitation. A typical feature of the magnetic excitation is a smooth phase variation with passing through zero, while electric excitation of the DR is characterized by an abrupt phase variation.

The capabilities of the broadband matching with magnetically excited single split-ring resonators with two splits are demonstrated in Figs. 6a–6c. Figure 6a shows the experimental frequency dependences of the reflection coefficient R of an absorber with single split-ring resonators (curve *1*') in comparison with the free absorber (curve *1*). A reduction in reflection is observed at frequencies above the resonance maximum of the reflection coefficient R of free rings (see Fig. 5a). Figure 6b shows the results of the calculation that qualitatively confirm the experiment and indicate a significant reduction in reflection from the metastructure with rings (curve *1*') in comparison with the free absorber (curve *1*). Introducing capacitances into the splits makes it possible to shift the resonances and change the matching conditions. In particular, Fig. 6c shows the measured frequency dependences of R for different metastructures using ring resonators loaded with 0.1-pF capacitances (curves *1*'–*3*') in comparison with the corresponding absorbers without rings (curves *1*–*3*). The broadband dips of reflection from the metastructures can be explained by reaching the matching due the possibility of adjusting the values of the parameter. The reflection is reduced by more than 15 dB in comparison with free absorbers.

Similar experiments were carried out for metastructures of split-ring resonators with four splits. To observe resonant effects in the given frequency range, capacitances of 0.1 pF were introduced into the splits of the rings (Fig. 1a). Figure 7a shows the frequency dependence of R for such a ring placed into a waveguide in orientation ***1*** (magnetic excitation). As can be seen from Fig. 7b, the reflection from the absorber with a ring resonator having orientation ***1*** (curve *1*') decreases in comparison with the free absorber (curve *1*).

3. PLANAR 1.5-TURN SPIRALS

Let us describe the succession of actions within the proposed method of measuring. We measure the frequency dependence of the transmission coefficient T and reflection coefficient R of a series of six planar 1.5-turn spirals, depending on their orientation relative to

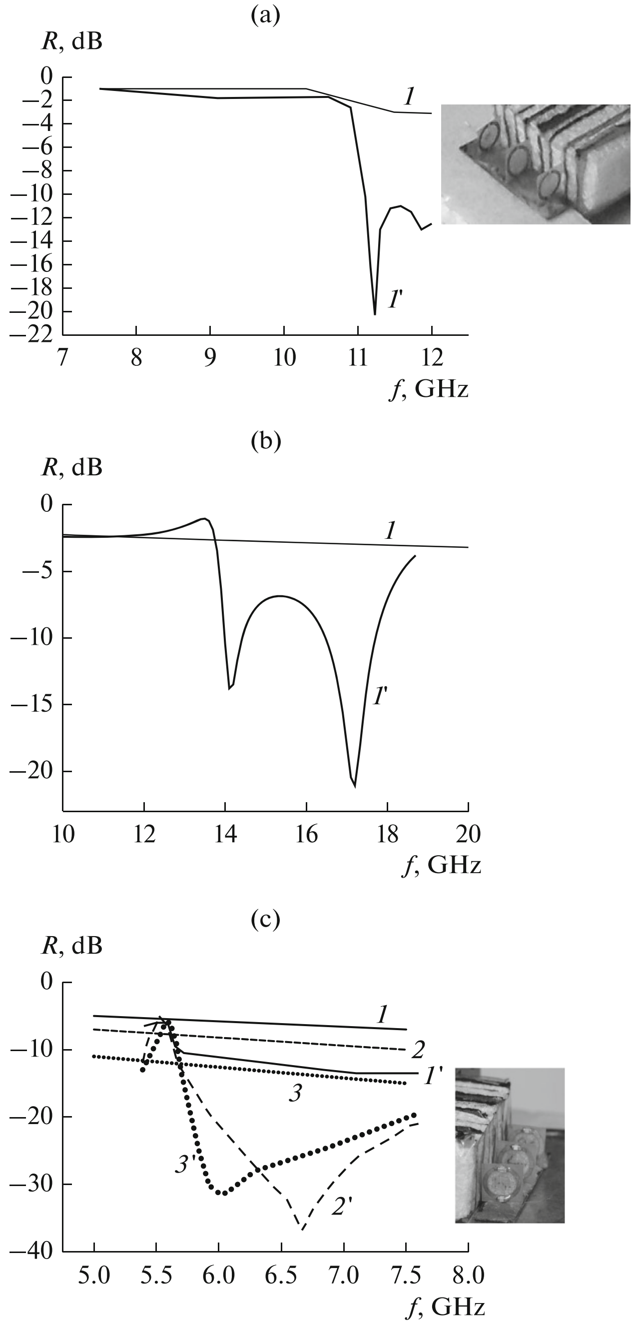

Fig. 6. Frequency dependences of reflection coefficient R of absorbers with single split-ring resonators ($1'$–$3'$) in comparison with free absorbers without rings (1–3): (a) experiment in a rectangular waveguide; (b) calculation in free space; (c) an experiment with ring resonators loaded with 0.1-pF capacitors.

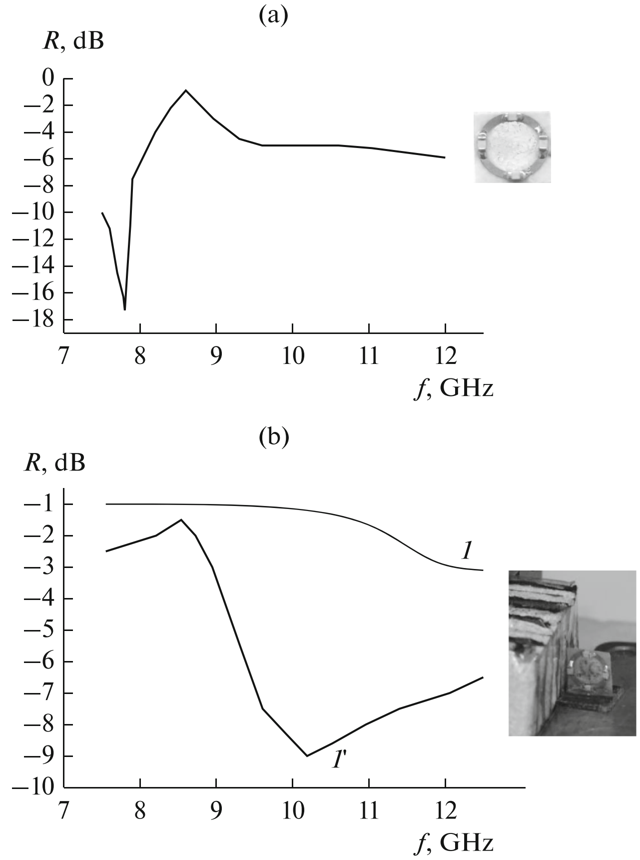

Fig. 7. Experimental frequency dependences of the reflection coefficient R: (a) of a single split-ring resonator with four splits loaded with 0.1-pF capacitors; (b) of an absorber ($1'$) with a ring in comparison with (1) an absorber without a ring.

the incident field components. We find orientations ***1*** and ***4*** (Fig. 8a), which are characterized by frequency dependences corresponding to magnetic and electrical excitation of RR at a frequency of 4.2 GHz (Fig. 8b) and electric excitation of the DR at 11.5 GHz (see Fig. 7c). Under the excitation of the RR, we observe a resonance maximum of reflection near 4.2 GHz and a resonant minimum, the position of which relative to the maximum depends on the orientation of the spirals (the type of excitation). In particular, in the traveling-wave mode in orientation ***1***, the minimum is observed below the frequency of the maximum and a large value of the reflection coefficient persists at higher frequencies, which corresponds to the magnetic excitation, while, in orientation ***4***, the minimum is observed near 5 GHz, i.e., above the resonance maximum, which corresponds to electric excitation. In the standing-wave mode, if spirals are placed on a metal plug (at the maximum of the magnetic field), in orientation ***1***, we observe a resonance dip of $R_{m,0}$, which disappears when the spirals are placed at a distance of $s = \lambda/4$, which is also typical of magnetic excitation. In addition, in orientation ***1***, we observe a DR at a frequency of 11.5 GHz (Fig. 8c) with indications of electric excitation. In particular, in the traveling-wave mode, the minimum of R is observed below the maximum and, in the standing-wave mode, a dip of the resonance reflection, $R_{m,\lambda/4}$, is observed if spirals are placed at a distance of $\lambda/4$ from the metal plug and is not observed at $s = 0$ ($R_{m,0}$). The possibility of matching

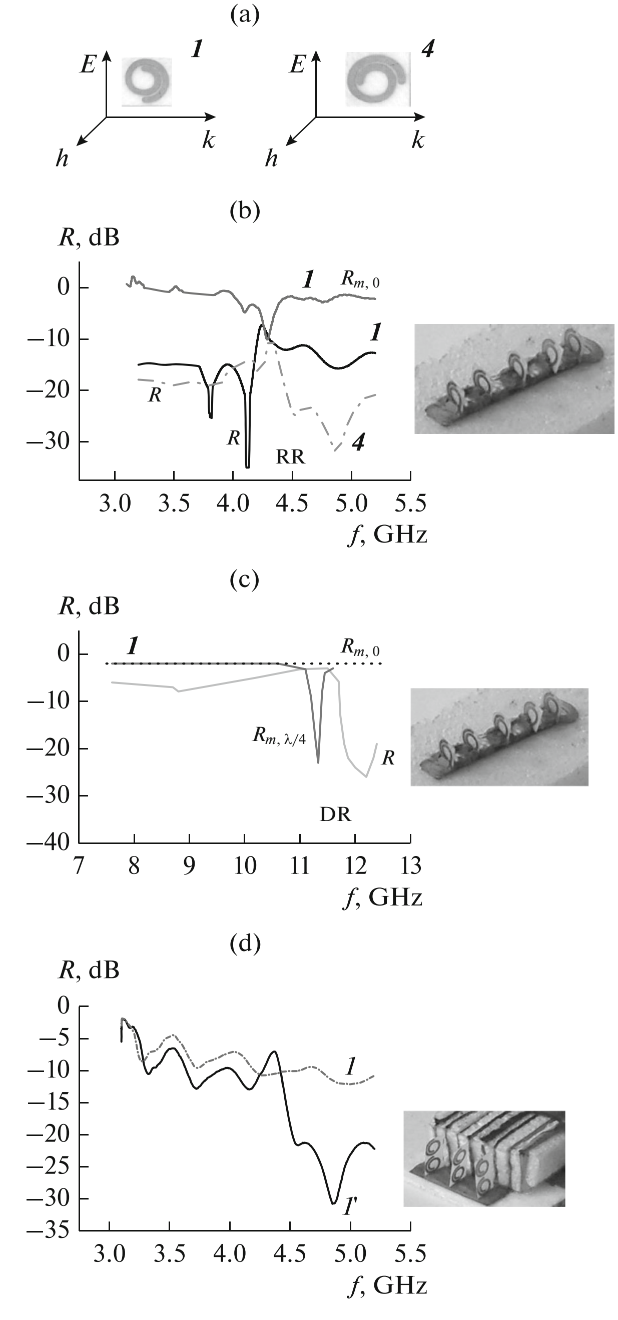

Fig. 8. (a) Orientations ***1*** and ***4*** of a planar 1.5-turn spiral relative to the wave vector k and the fields h and E of the incident electromagnetic wave; (b–d) experimental frequency dependences of the reflection coefficient: (b, c) of a chain of 5 spirals in the traveling-wave mode, R, and in the standing-wave mode, $R_{m,0}$ ($s = 0$) and $R_{m,\lambda/4}$ ($s = \lambda/4$) and in the region of the (b) RR and (c) DR; (d) of the absorber with planar 1.5-turns spirals (*1'*) in comparison with (*1*) the absorber without spirals.

with the use of magnetically excited planar spirals is evidenced by the results of measurements presented in Fig. 8d for the reflection coefficients of a metastructure containing an absorber and an array of rows of 1.5-turn spirals (curve *1'*) and for the absorber without matching spirals (curve *1*).

CONCLUSIONS

Ring elements of foil-coated polyamide film and layered radio-absorbing composites were produced by photolithography methods. Microwave responses of reflections in rectangular waveguide from double split-ring resonators (PDSRRs), single split-ring resonators with two and four splits, planar 1.5-turn spirals, and also responses of rings and spirals with radio absorbers in comparison with free absorbers without rings and spirals have been studied experimentally. The frequency dependences of the absolute values and phase of the reflection coefficients R of an infinite array of PDSRRs, of an array of single split-ring resonators, and array of single split-ring resonators with an absorber in comparison with the free absorber without an array have been obtained numerically.

The distinctive features of the frequency reflective characteristics of the magnetic and electric microwave responses, making it possible to reveal the magnetic response of inclusions of a wide variety of shapes, have been found. This is required not only for the development of metamaterials with artificial magnetism, "left-handed media", and their applications, but also opens up a new line of research aimed at the possibility of using the magnetic response for the broadband compensation of reflections from traditional absorbing composites based on resistive filaments or films.

It has been shown that, in addition to the resonant reflection maximum, conductive chiral and ring elements have an associated resonance minimum, the position of which depends on the orientation of the element (the type of excitation). Under magnetic excitation, this minimum is found below the frequency of the maximum, and, under electric excitation, it is found above this frequency. In this case, under magnetic excitation, the phase of the reflection coefficient varies smoothly, passing through zero, while, under electric excitation, the phase changes abruptly. In addition, magnetic excitation is characterized by a significant level of reflection in a wide frequency range above the frequency of the maximum. Therefore, it is possible to provide reflections, close in the amplitude and opposite in the phase, from the absorber and a closely placed array of resonant elements, excited by the magnetic field of the incident wave, i.e., the compensation of reflections from the absorber.

REFERENCES

1. Yu. V. Gulyaev, A. N. Lagar'kov, and S. A. Nikitov, Vestn. Ros. Akad. Nauk **78**, 438 (2008).
2. V. G. Veselago, Sov. Phys. Usp. **10**, 504 (1968).
3. D. R. Smith, W. J. Padilla, D. C. Vier, et al., Phys. Rev. Lett. **84**, 4184 (2000).

4. V. K. Varadan, V. V. Varadan, and A. Lakhtakia, J. Wave-Mater. Interact. **2** (1), 71 (1987).
5. T. Robin, B. Souillard, R. Accolas, et al., in Proc. 3rd Int. Workshop on Chiral, Bi-isotropic and Bi-anisotropic Media (CHIRAL'94), Perigueux, France, May 18–20, 1994 (Springer, Dordrecht, 1994), p. 103.
6. C. F. Bohren, R. Luebbers, H. S. Langdon, and F. Hunsberger, Appl. Opt. **31**, 6403 (1992).
7. V. S. Asadchy, I. A. Faniayeu, Y. Ra'dy, et al., Phys. Rev. **X 5**, 031005 (2015).
8. Q. Songsong, V. A. Bannyi, A. L. Samofalov, et al., Probl. Fiz., Mat. Tekh., No. 4, 40 (2014).
9. A. N. Lagar'kov, V. N. Kisel', and V. N. Semenenko, J. Commun. Technol. Electron. **57**, 1122 (2012).
10. N. Katsarakis, T. Koschny, M. Kafesaki, et al., Appl. Phys. Lett. **84** (15), 2943 (2004).
11. G. A. Kraftmakher and Y. N. Kazantsev, *Adv. Comp. Electromag. Mater., NATO ASI Series, Ser. 3* ***28***, Ed. by A. Priou, (Kluwer Academic, Dordrecht, 1997), p. 341.
12. D. R. Smith, S. Schultz, P. Markos, and C. M. Soukoulis, Phys. Rev. B **65**, 195104 (2002).
13. Yu. N. Kazantsev and G. A. Kraftmakher, Pis'ma Zh. Tekh. Fiz. **19** (11), 665 (1993).
14. Yu. N. Kazantsev, G. A. Kraftmakher, and V. P. Mal'tsev, Tech. Phys. Lett. **42**, 238 (2016).
15. Yu. N. Kazantsev, G. A. Kraftmakher, and V. P. Mal'tsev, J. Commun. Technol. Electron. **61**, 614 (2016).
16. Yu. N. Kazantsev and V. N. Apletalin, J. Commun. Technol. Electron. **52**, 390 (2007).
17. B. Y. Zhang, J. Hendrickson, and N. Nader, et al., Appl. Phys. Lett. **105**, 241113 (2014).
18. R. Marques, F. Medina, and R. Rafii-El-Idrissi, Phys. Rev. B **65**, 144440 (2002).
19. B. Sauviac, C. R. Simovski, and S. A. Tretyakov, Electromagnetics **24**, 317 (2004).
20. V. S. Butylkin, G. A. Kraftmakher, and V. P. Mal'tsev, J. Commun. Technol. Electron. **54**, 1124 (2009).
21. M. V. Kostin, Yu. N. Kazantsev, G. A. Kraftmakher, and V. V. Shevchenko, Pis'ma Zh. Tekh. Fiz. **16** (13), 22 (1990).
22. Yu. N. Kazantsev, M. V. Kostin, and G. A. Kraftmakher, Radiotekh. Elektron. (Moscow) **39**, 1652 (1994).
23. V. S. Butylkin and G. A. Kraftmakher, J. Commun. Technol. Electron. **53**, 1 (2008).
24. M. V. Kostin and V. V. Shevchenko, in *Proc. 3rd Int. Workshop on Chiral, Bi-isotropic and Bi-anisotropic Media (CHIRAL'94), Perigueux, France, May 18–20, 1994* (Springer, Dordrecht, 1994), p. 49.
25. V. S. Butylkin and G. A. Kraftmakher, J. Commun. Technol. Electron. **51**, 484 (2006).

Translated by E. Chernokozhin